Title

CDK4/6 and IGF1 Receptor Inhibitors Synergize to Suppress the Growth of p16INK4A-Deficient Pancreatic Cancers

Journal

Cancer Research, 74(14)

ISSN

0008-5472

Authors

Heilmann, Andreas M
Perera, Rushika M
Ecker, Veronika
et al.

Publication Date

2014-07-15

DOI

10.1158/0008-5472.can-13-2923

Peer reviewed

Published in final edited form as:
Cancer Res. 2014 July 15; 74(14): 3947–3958. doi:10.1158/0008-5472.CAN-13-2923.

CDK4/6 and IGF1 receptor inhibitors synergize to suppress the growth of p16INK4A-deficient pancreatic cancers

Andreas M. Heilmann, **Rushika M. Perera**, **Veronika Ecker**, **Brandon N. Nicolay**, **Nabeel Bardeesy**, **Cyril H. Benes**, and **Nicholas J. Dyson**
Massachusetts General Hospital Cancer Center, Harvard Medical School, Building 149, 13th Street, Charlestown, MA, 02129, USA

Abstract

Loss-of-function mutations in $p16^{INK4A}$ (*CDKN2A*) occur in approximately 80% of sporadic pancreatic ductal adenocarcinoma (PDAC), contributing to its early progression. While this loss activates the cell cycle-dependent kinases CDK4/6, which have been considered as drug targets for many years, $p16^{INK4A}$-deficient PDAC cells are inherently resistant to CDK4/6 inhibitors. This study searched for targeted therapies that might synergize with CDK4/6 inhibition in this setting. We report that the IGF1R/IR inhibitor BMS-754807 cooperated with the CDK4/6 inhibitor PD-0332991 to strongly block proliferation of $p16^{INK4A}$-deficient PDAC cells *in vitro* and *in vivo*. Sensitivity to this drug combination correlated with reduced activity of the master cell growth regulator mTORC1. Accordingly, replacing the IGF1R/IR inhibitor with the rapalog inhibitor temsirolimus broadened the sensitivity of PDAC cells to CDK4/6 inhibition. Our results establish targeted therapy combinations with robust cytostatic activity in $p16^{INK4A}$-deficient PDAC cells and possible implications for improving treatment of a broad spectrum of human cancers characterized by $p16^{INK4A}$ loss.

Keywords

PD-0332991; palbociclib; BMS-754807; PDAC; drug synergy

Introduction

The retinoblastoma tumor suppressor (pRB) pathway is a key negative regulator of cell proliferation and functionally inactivated in many cancers (1). During the G1 phase of the cell cycle, cyclin-dependent kinases phosphorylate pRB, allowing E2F transcription factors to drive S-phase entry and to promote cell cycle progression (2). The regulation of pRB is frequently compromised in tumor cells by loss of the *CDKN2A* locus (3). *CDKN2A* encodes $p16^{INK4A}$, an inhibitor of CDK4 and CDK6, and $p14^{ARF}$, an inhibitor of MDM2-mediated p53 degradation (4). Loss of $p16^{INK4A}$ results in hyperactive Cyclin D-CDK4/6 kinase complexes and pRB is the best known member of a plethora of CDK4/6 substrates (5). In

Corresponding Author: Nicholas J. Dyson, Massachusetts General Hospital Cancer Center, Harvard Medical School, Building 149, 13th Street, Charlestown, MA, 02129, USA. 617-726-7804 (phone), 617-726-7808 (fax), dyson@helix.mgh.harvard.edu.

Conflict of interest: The authors disclose no potential conflicts of interest.

normal cells, Cyclin D-CDK4/6 kinases integrate mitogenic signals. Elevated CDK4/6 activity promotes tumor growth by counteracting tumor suppressor mechanisms, such as senescence and apoptosis (6–8). Since the great majority of cancers with *CDKN2A* loss retain intact *RB1*, there is considerable interest in targeting CDK4/6 as a treatment strategy for these tumors, and in identifying drug combinations that potentiate the therapeutic effect.

PD-0332991 (palbociclib) is an orally active CDK4/6 specific inhibitor, which selectively inhibits CDK4 and CDK6 with *in vitro* IC50s of 11 nM and 16 nM, respectively (9). In cells that express intact pRB, PD-0332991 blocks pRB phosphorylation at sites normally targeted by CDK4/6 (including serines S807/811 and S780) and causes G1 cell cycle arrest (9,10). PD-0332991 has been well tolerated in phase I clinical trials and is effective in mantle cell lymphoma as well as in estrogen receptor (ER)-positive luminal breast cancer (10–13). By contrast, single agent treatment with PD-0332991 has produced only modest responses in most other malignancies regardless of *CDKN2A* mutational status.

The mechanisms of resistance to PD-0332991 in tumors predicted to have hyperactive CDK4/6 are poorly understood. Mutant forms of pRB that lack CDK phosphorylation sites give a dominant arrest in tumor cell lines (14). A combination of PD-0332991 and drugs that converge on the pRB pathway might lead to more effective CDK4/6 suppression and more stable pRB reactivation. Indeed recent preclinical studies have shown CDK4/6 inhibition to cooperate with therapeutics targeting oncogenic drivers of $p16^{INK4A}$-mutant cancers, such as pediatric astrocytoma and malignant melanoma (15,16).

Pancreatic ductal adenocarcinoma (PDAC) is the fourth leading cause of cancer death in the United States and highly resistant to existing treatments. Since *CDKN2A* inactivation occurs in 80-95% of cases and contributes to the early progression of PDAC precursor lesions, whereas *RB1* remains intact, CDK4/6 is an attractive target in these tumors (17–21). Here we sought to identify compounds showing synergy with CDK4/6 inhibitors in PDAC. Analysis of a comprehensive screen identifying genomic markers for drug sensitivities in cancer cell lines (22) suggested that mutational status of *CDKN2A* may correlate with sensitivity to inhibitors that selectively target the insulin-like growth factor I receptor (IGF1R) and the related insulin receptor (IR). We found that concurrent targeting of CDK4/6 and IGF1R/IR resulted in synergistic effects on proliferation of *CDKN2A*-mutant PDAC cell lines *in vitro* and potent suppression of tumor growth *in vivo*. pRB depletion or activation of the key IGF1R/IR downstream effector mTORC1 were sufficient to render cells resistant to the synergistic drug combination, suggesting that alterations in these pathways converge to promote the growth of *CDKN2A*-deleted PDAC cells.

Materials and Methods

Cell lines and drugs

All cell lines were provided and authenticated by The Center of Molecular Therapeutics (Massachusetts General Hospital Cancer Center) and cultured in RPMI medium containing 5% fetal bovine serum (FBS), except for YAPC, HPAC, HPAF-II, and Panc1, which were grown in DMEM with 10% FBS, and MIA-PaCa-2, which was grown in DMEM/F12 with 5% FBS. Cell media were supplemented with penicillin/streptavidin and glutamine, and

cells were maintained at 37 °C and 5% CO_2. BMS-754807, OSI-906, and PD-0332991 were purchased from ChemieTek, temsirolimus and AZD8055 were from Selleck Chemicals. The compounds used to treat cells were dissolved in DMSO at 10 mM and stored at -80 °C.

Cell viability and synergy assays

Cells were seeded in 96-well plates at 2000-4000 cells/well depending on the growth characteristic of the cell line so that each was in growth phase at the end of the assay (60-80% confluency). The following day, cells were treated in duplicate with single agents and their fixed-ratio combination for 72 h over an 8-point, 128-fold concentration range, which was centered on the single agent concentrations that inhibited viability by 50% (IC50). Cell viability was measured by staining the cells for 4 h with 100 μg/ml resazurin (Sigma) whose conversion was detected at wavelengths of 510/595 nM using a SpectraMax® M5 plate reader (Molecular Devices). The R software package *mixlow* (23) was applied to derive Loewe synergy indexes from the sensitivities to the single agents and their combination.

Mouse treatment study

One million YAPC cells in 100 μl PBS were injected subcutaneously into each flank of 10-week old female CB17/lcr-Prkdc^{scid}/lcrCrl mice (Charles River Laboratories). After one week, tumor volumes were determined using electronic calipers to measure the length (L) and width (W) and calculated according to the formula (LxW^2)/2. The mice were separated into four groups matched for tumor volume (50-60 mm^3), which were randomly assigned to treatment arms. For oral administration, BMS-754807 was dissolved in sterile polyethylene glycol 400 (PEG400)/water (4:1, v/v) and PD-0332991 was dissolved in sterile 50 mM sodium lactate (pH 4). The drugs or their vehicles were administered by gastric gavage every other day starting from day 8 post injection, with PD-0332991 at 75 mg/kg being fed in the morning and BMS-754807 at 15 mg/kg in the evening (minimum of 6 h between PD-0332991 and BMS-754807). Tumor volumes were assessed twice weekly as described above. For pharmacodynamic evaluation at the study endpoint, tumor tissue was harvested 3 h after the final BMS-754807 dose and frozen in liquid nitrogen or fixed in 10% formalin. All mouse studies were conducted through Institutional Animal Care and Use Committee (IACUC #2005N000148) approved animal protocols in accordance with institutional guidelines.

Additional Materials and Methods are described in the Supplementary Methods.

Results

CDK4/6 and IGF1R/IR inhibitors synergize in *CDKN2A*-deleted PDAC lines

To identify targeted therapies that sensitize cancer cells to the CDK4/6 inhibitor PD-0332991, we examined drug sensitivity data from a comprehensive cancer cell line screen (22). As expected, sensitivity to PD-0332991 was associated with *CDKN2A* loss and lack of *RB1* mutations. We noted that *CDKN2A* was the cancer gene whose mutational status most frequently correlated with differential drug response [supplementary figure 4 of reference (22)]. The correlations with *CDKN2A* status were particularly evident in PDAC

cell lines where 32 drugs showed a trend towards decreased efficacy in the context of mutant *CDKN2A* versus wild-type *CDKN2A*. However, the number of *CDKN2A* wild-type PDAC lines included in the screen was small (N=3), thus any hypothesis coming from this data needed to be verified experimentally. We reasoned that if the difference in drug sensitivity was indeed associated with inactivation of *CDKN2A* then it should be possible to recapitualte this effect by combining these drugs with PD-0332991 in *CDKN2A*-mutant PDAC cells, since this would mimic functional $p16^{INK4A}$ (Figure S1).

The drugs with decreased sensitivities in *CDKN2A*-mutant PDAC cells included three different small molecule IGF1R/IR kinase inhibitors (Supplementary Table S1 and Figure S2). BMS-754807, with *in vitro* IC50s of less than 2 nM for IGF1R/IR, is the most potent of these compounds (24). IGF1R and IR are receptor protein tyrosine kinases that upon ligand binding phosphorylate insulin receptor substrate (IRS) proteins, which activate the PI3K-AKT-mTOR as well as the RAS-MAPK signaling axes (25), key effectors in oncogenic *KRAS*-driven PDAC development (26).

To test whether targeting of CDK4/6 sensitizes PDAC cells to IGF1R/IR inhibitors, we employed a Loewe synergy assay, which allows for testing of drug combinations in fixed ratios (23). PDAC cells were treated with PD-0332991, BMS-754807 and their combination over an 8-point, 128-fold concentration range for 72 h and viability was measured with resazurin. The combination of PD-0332991 and BMS-754807 reduced viability of the PDAC cell line MIA-PaCa-2 significantly at doses that had comparatively minor effects in the single agent treatments (Figure 1A). The combination of PD-0332991 with a second IGF1R/IR inhibitor (OSI-906) resulted in similar sensitivities (Figure 1B), suggesting that the effects of the drug combination are due to on-target IGF1R/IR inhibition (Figure S3). To confirm that loss of CDK4/6 activity sensitizes the cells to IGF1R/IR inhibitors, we treated MIA-PaCa-2 cells with BMS-754807 after CDK4, CDK6 or CDK4 and CDK6 had been depleted with siRNAs (Figure 1C). Of note, depletion of CDK4 and CDK6 decreased MIA-PaCa-2 viability by 60%, indicating that these $p16^{INK4A}$-mutant cells rely on CDK4/6 for growth. BMS-754807 significantly reduced viability of cells treated with siRNAs targeting CDK4 or CDK4 and CDK6, but did not affect cells treated with control siRNA or CDK6 siRNA. These data suggest that targeting of CDK4/6 sensitizes PDAC cells to IGF1R/IR inhibition and thus cooperates to reduce PDAC cell viability.

Next we carried out a systematic assessment of drug synergy across a panel of PDAC cell lines. Loewe synergy indexes were derived from the sensitivities to the single agents and their combination using the R software package *mixlow* (23) in fourteen PDAC cell lines, including lines with homozygous *CDKN2A* deletion, *CDKN2A* point mutations and wild-type *CDKN2A* (Figure 1D and S4). BMS-754807 (15-500 nM) and PD-0332991 (0.15-5.0 μM) synergized significantly to reduce viability up to 70-80% in the cell lines MIA-PaCa-2, PSN1, HuP-T3, and YAPC and showed synergy limited to a part of the effect range in the HPAC and AsPC-1 lines (Figure 1E). No synergy was observed at high doses (PD-0332991 > 10 μM), most likely due to off-target drug effects.

All cell lines susceptible to the drug synergism harbor deletions that span the *CDKN2A* locus and frequently affect adjacent genes (Sanger COSMIC Cell Line Project). To assess

the potential role of these co-deleted genes, the drug synergy status of the cell lines was compared with their *CDKN2A*, *MTAP*, and *CDKN2B* mRNA expression levels (Broad-Novartis Cancer Cell Line Enzyclopedia). While *CDKN2A* expression is lost in all four susceptible lines (Figure 1F), PSN1 cells have detectable *CDKN2B* mRNA, and YAPC express *MTAP* (Figure S5), suggesting that CDKN2A loss is the primary requirement for the drug synergy. Of note, *CDKN2A* loss is not sufficient to generate sensitivity to the drug combination. Since $p16^{INK4A}$ is frequently lost by means other than genetic deletion, we used siRNA against CDK4/6 to verify that the proliferation of two sensitive lines depends on CDK4/6, while the proliferation of two *CDKN2A* wild-type lines does not (Figure 1G). In conclusion, we have identified a drug combination that synergistically inhibits viability in more than half (4/7) of the *CDKN2A*-deleted PDAC cell lines tested.

Concurrent inhibition of CDK4/6 and IGF1R/IR enhances G1-arrest and senescence

Cyclin D-CDK4/6 kinase complexes drive G1-S cell cycle progression. We performed cell cycle analysis to examine how the CDK4/6 inhibitor affects viability when combined with IGF1R/IR inhibitor. Treatment of MIA-PaCa-2 cells with PD-0332991 for 24 h resulted in an increased G1/0 population (from 41% to 61%) and reductions in the proportion of cells in S-phase (45% to 30%) and G2/M (14% to 8%) (Figure 2A). In combination with BMS-754807, G1/0 arrest was markedly augmented (15% S, 77% G1/0, and 7% G2/M), whereas BMS-754807 alone did not significantly affect cell cycle distribution (Figure 2A). To determine the timing of this enhanced G1/0 arrest, we investigated shorter treatment durations. PD-0332991 reduced the S-phase population more potently to 13% and 10% after 8 and 16 h, respectively (Figure 2B). BMS-754807 addition decreased this fraction further to 4% at 16 h, but had no added effect at 8 h. These data suggest that IGF1R/IR inhibition synergizes with CDK4/6 inhibition by enhancing the PD-0332991 induced G1/0 arrest starting from 16 h after addition of the drugs and by maintaining the G1-S block more efficiently. The enhanced G1/0 arrest at 24 h was confirmed for the sensitive PSN1, HuP-T3, and YAPC lines (Figure 2C).

Prolonged G1/0 arrest can lead to senescence and PD-0332991 has previously been shown to cause senescence in solid tumors (6). Correspondingly, staining for senescence-associated β-galactosidase (SA-β-gal) (27), revealed that combination treatment induced high levels of senescence compared with the single agents (combination treatment 61% SA-β-gal positive cells versus BMS-754807 13% and PD-0332991 42%) (Figure 2D). Comparable results were obtained for HuP-T3 and YAPC cells, in which the drug combination induced a significant increase of SA-β-gal. These findings were further corroborated by counting population doublings of HuP-T3 and YAPC cells cultured in the presence of the inhibitors and passaged every four days. Combination treatment prevented population doubling in HuP-T3 cells and strongly slowed it in YAPC cells treated with half the drug doses compared to the HuP-T3 experiments, consistent with induction of a cytostatic senescence response, whereas BMS-754807 had no significant effect on cell proliferation and PD-0332991 showed an intermediate effect (Figure 2E).

Combined CDK4/6 and IGF1R/IR inhibition is synergistic *in vivo*

We evaluated whether combined CDK4/6 and IGF1R/IR inhibition is synergistic *in vivo* and could be a potential therapeutic approach against PDAC. Xenograft tumors were generated with YAPC cells, which are sensitive to the drug combination *in vitro* and form tumors within a week after subcutaneous injection into SCID mice. Once tumors reached 50 mm^3 in volume, the mice were grouped and treatment was initiated with submaximal tolerated doses of each inhibitor. Administration of the single agents had no significant effect on the tumor volume, paralleling the *in vitro* results (Figure 3A). In contrast, the combination therapy slowed tumor growth approximately 2.5-fold and significantly reduced tumor burden as compared to both the vehicle and the monotherapy cohorts (Figure 3A), suggesting that concurrent targeting of CDK4/6 and IGF1R/IR is synergistic *in vivo*. This efficacy was achieved in the absence of any apparent adverse effects. Consistent with the *in vitro* findings, we observed increased staining for the senescence marker trimethylated lysine 9 histone H3 in PD-0332991 treated tumors, which was further enhanced by the drug combination (Figure S6).

To confirm that the drugs inhibited their respective targets *in vivo*, we analyzed the tumors at the study endpoint for CDK4/6 and IGF1R/IR signaling. BMS-754807 alone or in combination with PD-0332991 reduced tyrosine autophosphorylation of IGF1R/IR as well as phosphorylation of the IGF1R/IR downstream effector AKT (Figure 3B). Single agent PD-0332991 did not affect these phosphorylation events. To read out the activity of mechanistic target of rapamycin complex 1 (mTORC1) downstream of IGF1R/IR-AKT, we detected S6K1 phosphorylation at the mTORC1 site T389. While BMS-754807 alone had only a slight effect, the drug combination abrogated S6K1 phosphorylation, suggesting that IGF1R/IR-AKT inhibition only translated to effective mTORC1 suppression in the presence of the CDK4/6 inhibitor, which did not decrease S6K1 activation by itself. To evaluate CDK4/6 activity in the tumors, we detected pRB phosphorylation at the CDK4/6 sites S807/811. The drug combination notably reduced phospho-pRB levels, whereas either single agent treatment led to a minimal decrease in pRB phosphorylation. In accordance with a previous study noting that PD-0332991 stabilizes Cyclin D1 (28), we observed elevated Cyclin D1 levels in tumors that had been treated with the CDK4/6 inhibitor alone or in combination, indicating that PD-0332991 targeted CDK4/6 in both regimes. *In vitro* experiments confirmed that BMS-754807 enhances PD-0332291 mediated inhibition of pRB phosphorylation in YAPC cells even under conditions optimal for drug delivery (Figure S7). Together, these data indicate that the single agents affected their respective targets, but did not suppress tumor growth. In contrast, the drug combination elicited a tumorstatic response corresponding with enhanced S6K1 inhibition and pRB reactivation.

The drug combination specifically reduces S6K1 phosphorylation

To elucidate the mechanistic basis for the drug synergy, we investigated the phosphorylation of the CDK4/6 substrate pRB and of IGF1R/IR effectors after addition of BMS-754807, PD-0332991 and their combination. PSN1 cells were treated with PD-0332991, which abrogated pRB phosphorylation 16 h after drug addition (Figure 4A). This effect was not present at time points as early as two hours, most likely due to the fact that asynchronously cycling cell populations were used. CDK4/6 inhibition was combined with low doses of

BMS-754807 that dampened AKT activation in a dose-dependent manner (Figure 4A). As observed in the xenograft tumors, BMS-754807 mediated inhibition of S6K1 T389 phosphorylation was enhanced by PD-0332991 (Figure 4A). Thus, these compounds cooperate to inactivate mTORC1 in PDAC cells *in vitro* and *in vivo*.

To address whether this effect may be responsible for the drug synergy, we compared the effects on S6K1 phosphorylation in two lines that displayed the synergy with two lines that did not show the synergistic effects. While concurrent treatment with BMS-754807 and PD-0332991 significantly reduced S6K1 phosphorylation in the sensitive MIA-PaCa-2 and HuP-T3 cell lines (Figure 4B), it had no effect in PANC-03-27 or CFPAC-1 cells, in which the inhibitors do not synergize. The inhibitors did not affect ERK1/2 activity suggesting that the signaling alterations were specific to the PI3K-mTOR pathway (Figure 4B).

Cylin D1 or CDK4/6 depletion sensitizes PDAC cells to S6K1 inhibition

The cooperation of CDK4/6 inhibitor with IGF1R/IR targeting on the level of mTORC1 raised the question whether this effect of PD-0332991 was through inhibition of CDK4/6 or off-target. To distinguish between these possibilties, Cyclin D1 or CDK4/6 were depleted with siRNA followed by BMS-754807 treatment for 2 h. Cyclin D1 knock-down sensitized MIA-PaCa-2 and YAPC cells to BMS-754807 mediated inhibition of S6K1 phosphorylation (Figure 5A). Identical results were obtained in YAPC cells after CDK4/6 depletion. CDK4/6 knock-down in MIA-PaCa-2 cells lead to increased phospho-S6K1 that was strongly reduced by BMS-754807, which had no effect on control siRNA transfected cells (Figure 5B). These findings indicate that the PD-0332991 mediated sensitization to mTORC1 inhibition is specific and could thus be shared by other CDK4/6 inhibitors.

CDK4/6 and mTOR inhibitors synergize in *CDKN2A*-deleted PDAC lines

The observed effect on phosphorylation of S6K1, a primary substrate of mTORC1, raised the question whether mTORC1 inhibition would suffice to synergize with CDK4/6 inhibition. Indeed, PD-0332991 synergized with temsirolimus, an allosteric mTOR inhibitor that specifically targets mTORC1, to reduce viability of not only the PDAC lines sensitive to BMS-754807/PD-0332991, but also the additional lines PANC-03-27, BxPC-3 and PANC-10-05 (Figure 6A and S8). IGF1R/IR signaling may not be required for mTORC1 activity in these lines. Remarkably, combined CDK4/6 and mTORC1 inhibition synergized, at least partially, in all of the *CDKN2A*-deleted PDAC lines tested (Figure 6B).

Catalytic mTOR kinase inhibitors, such as AZD8055, have recently been developed in order to target both mTOR complexes and abolish mTORC1 activities more effectively than rapalogs. AZD8055, which is two orders of magnitude more potent than temsirolimus in HuP-T3 cells, synergized with PD-0332991 (Figure 6C), indicating that the effects of these compounds can be further enhanced by concurrent CDK4/6 inhibition. This result excludes any catalytic off-target effects of PD-0332991 on mTOR kinase itself, as the combination of two catalytic mTOR inhibitors would have been expected to be additive, rather than synergistic.

TSC2 or pRB depletion restores growth in the presence of CDK4/6 and IGF1R/IR inhibitors

To evaluate the role of mTORC1 in mediating the synergistic drug effects, we performed sensitivity assays with cells after knockdown of tuberous sclerosis 2 (TSC2). TSC2 is an integral part of the tuberous sclerosis complex and incorporates signaling inputs from AKT, RSK, nutrient and stress signaling to restrain mTORC1 activity. TSC2 depletion in three different cell lines (PSN1, MIA-PaCa-2, and HuP-T3) restored cell proliferation in the presence of PD-0332991 and BMS-754807/PD-0332991 (Figure 7A), suggesting that mTORC1 activation is sufficient to render cells resistant to the CDK4/6 inhibitor and the combination therapy. This effect was specific to the combination of CDK4/6 and IGF1R/IR inhibitors, as TSC2 depletion did not completely prevent growth inhibition in the presence of PD-0332991 and temsirolimus, which blocks mTORC1 downstream of TSC2 (Figure 7A).

The best-established Cyclin D-CDK4/6 substrates are the pRB family members. Since pRB fulfills a unique role among the pocket proteins in mediating oncogene-induced senescence, we tested whether loss of pRB would render cells insensitive to the synergistic drug combination. We made stable MIA-PaCa-2 and HuP-T3 lines, in which pRB was depleted with two different shRNAs, and determined their sensitivities to BMS-754807, PD-0332991, and their combination. The pRB depleted cell pools were less sensitive to either drug alone as well as to the drug combination (Figure 7B), with the shRNA construct that gave the stronger reduction in pRB levels (shRB1-2) conferring a higher degree of resistance. These data suggest that both IGF1R/IR and CDK4/6 inhibitors engage the pRB tumor suppressor pathway and that pRB loss can alleviate the synergistic effects of the drug combination.

Discussion

Here we identify inherent resistance of *CDKN2A*-mutant PDAC cells to CDK4/6 inhibitor and describe drug combinations that efficiently reactivate the pRB tumor suppressor pathway to trigger cell cycle arrest and senescence. *CDKN2A* loss is frequent in PDAC and contributes to PDAC progression by bypassing oncogenic *RAS*-induced senescence (29–31). Although several *CDKN2A*-mutant PDAC cell lines indeed depend on CDK4/6, only one out of 13 cell lines with *CDKN2A* mutations is sensitive to PD-0332991 (AsPC-1 IC50 0.25 μM, Table S1). Our data suggest that *CDKN2A*-deleted PDAC cells are instrinsically resistant to CDK4/6 inhibition alone, since PD-0332991 failed to induce sustained growth arrest and senescence at concentrations that initially block CDK4/6 activity as evidenced by decreased pRB phosphorylation. This inherent resistance to PD-0332991 is likely due to elevated PI3K-mTOR activity. *KRAS*-driven PDAC formation and maintenance has been demonstrated to depend on active PI3K signaling (26) that suppresses oncogenic *RAS*-induced senescence in pancreatic cancer (30). The results described here show that targeting of IGF1R/IR, which potently inhibited the PI3K effector AKT, in combination with CDK4/6 inhibition resulted in prolonged cell cycle arrest and increased SA-β-gal activity *in vitro* as well as tumor stasis *in vivo*, in accordance with the drug combination reinstating oncogene-induced senescence.

Despite the evidence for IGF1R being an important target in PDAC, clinical trials with IGF1R-blocking antibodies have been disappointing (32). Our study provides evidence that

CDKN2A-mutant PDAC cells are inherently insensitive to IGF1R/IR inhibition alone. CDK4/6 has long been known for its role to promote growth in model organisms and its constitutive activation following $p16^{INK4A}$ loss may provide growth signals in the absence of IGF1R/IR signaling. Although the IGF1R/IR inhibitor BMS-754807 repressed AKT activation at low nanomolar doses, it failed to efficiently inhibit the mTORC1 substrate S6K1 at these concentrations and impacted viability only at doses that were two orders of magnitude higher. Persistent activation of mTOR has recently been described to correlate with resistance of breast cancers to PI3K inhibitor (33) as well as with resistance of melanoma to RAF or MEK inhibitor (34). Similarly, here we found that the response to concurrent CDK4/6 and IGF1R/IR inhibition correlated well with decreased mTORC1 activity. PD-0332991 mediated sensitization to mTORC1 inhibition could be recapitulated with siRNA against either Cyclin D1 or CDK4/6, suggesting that other CDK4/6 inhibitors could share this activity. Overexpressed Cyclin D has been previously shown to bind the mTORC1 negative regulator TSC2 (35), providing evidence of a direct physical connection between Cyclin D1-CDK4/6 and regulation of mTORC1. To date, we have been unable to confirm this interaction between the endogenous proteins. Our results do, however, suggest that TSC2 likely plays a critical role in this synergistic drug response, as its depletion rendered cells resistant to the combination of CDK4/6 and IGF1R/IR inhibitors. Furthermore, PD-0332991 synergized with the rapalog temsirolimus. This drug combination may be more easily translatable, since it expanded the number of sensitive *CDKN2A*-mutant lines and rapalogs have been well tolerated in clinical settings.

The synergistic effects seen by combining PD-0332991 with other treatments apply to other cancer types. A recent drug synergy screen and network modeling study suggested that hyperactive CDK4 and IGF1R signaling also cooperate in liposarcoma (36). Targeting additional cancer types may require the identification of context-specific oncogenic drivers that cooperate with CDK4/6 deregulation (37). Apart from the clinical benefit of a combination of PD-0332991 and letrozole seen in ER-positive breast cancer, several preclinical studies have shown PD-0332991 to be effective in combination with drugs targeting mitogenic drivers in pediatric astrocytoma, melanoma, and prostate cancer (15,16,28). In conclusion, our work suggests that *CDKN2A* loss in PDAC can be exploited by concurrent targeting of CDK4/6 and the IGF1R/IR-mTOR axis in order to efficiently reactivate pRB tumor suppressor functions and suppress growth.

Supplementary Material

Refer to Web version on PubMed Central for supplementary material.

Acknowledgments

We thank members of the Dyson laboratory for helpful discussions and Jennifer Spangle for critical reading of the manuscript. We also thank Per Hydbring and Peter Sicinski for the H3K9me3 staining protocol and antibody. This work was supported by the National Institutes of Health (NIH) Public Health Service grants R01 CA163698 and R01 CA155202 (to ND). Andreas Heilmann is supported by the Postdoctoral Fellowship PF-13-321-01-TBG from the American Cancer Society and Brandon Nicolay by the Postdoctoral Fellowship CA165856 from the NIH. Nicholas Dyson is the James and Shirley Curvey MGH Research Scholar.

Financial support: R01 CA163698 and R01 CA155202 (Dyson), PF-13-321-01-TBG (Heilmann), NIH/NRSA CA165856 (Nicolay)

References

1. Burkhart DL, Sage J. Cellular mechanisms of tumour suppression by the retinoblastoma gene. Nat Rev Cancer. 2008; 8:671–82. [PubMed: 18650841]
2. Weinberg, Ra. The retinoblastoma protein and cell cycle control. Cell. 1995; 81:323–30. [PubMed: 7736585]
3. Bignell GR, Greenman CD, Davies H, Butler AP, Edkins S, Andrews JM, et al. Signatures of mutation and selection in the cancer genome. Nature. 2010; 463:893–8. [PubMed: 20164919]
4. Serrano M, Lin AW, Mccurrach ME, Beach D, Lowe SW. Oncogenic ras Provokes Premature Cell Senescence Associated with Accumulation of p53 and p16 INK4a. Cell. 1997; 88:593–602. [PubMed: 9054499]
5. Anders L, Ke N, Hydbring P, Choi YJ, Widlund HR, Chick JM, et al. A systematic screen for CDK4/6 substrates links FOXM1 phosphorylation to senescence suppression in cancer cells. Cancer Cell. 2011; 20:620–34. [PubMed: 22094256]
6. Choi YJ, Li X, Hydbring P, Sanda T, Stefano J, Christie AL, et al. The requirement for cyclin d function in tumor maintenance. Cancer Cell. 2012; 22:438–51. [PubMed: 23079655]
7. Choi YJ, Anders L. Signaling through cyclin D-dependent kinases. Oncogene. 2013:1–14.
8. Brown NE, Jeselsohn R, Bihani T, Hu MG, Folotpoulou P, Kuperwasser C, et al. Cyclin D1 activity regulates autophagy and senescence in the mammary epithelium. Cancer Res. 2012; 72:6477–89. [PubMed: 23041550]
9. Fry DW, Harvey PJ, Keller PR, Elliott WL, Meade M, Trachet E, et al. Specific inhibition of cyclin-dependent kinase 4 / 6 by PD 0332991 and associated antitumor activity in human tumor xenografts Specific inhibition of cyclin-dependent kinase 4 / 6 by PD 0332991 and associated antitumor activity in human tumor xenografts. Mol Cancer Ther. 2004; 3:1427–38. [PubMed: 15542782]
10. Finn RS, Dering J, Conklin D, Kalous O, Cohen DJ, Desai AJ, et al. PD 0332991, a selective cyclin D kinase 4/6 inhibitor, preferentially inhibits proliferation of luminal estrogen receptor-positive human breast cancer cell lines in vitro. Breast cancer Res. 2009; 11:R77. [PubMed: 19874578]
11. Leonard JP, LaCasce AS, Smith MR, Noy A, Chirieac LR, Rodig SJ, et al. Selective CDK4/6 inhibition with tumor responses by PD0332991 in patients with mantle cell lymphoma. Blood. 2012; 119:4597–607. [PubMed: 22383795]
12. Schwartz GK, LoRusso PM, Dickson Ma, Randolph SS, Shaik MN, Wilner KD, et al. Phase I study of PD 0332991, a cyclin-dependent kinase inhibitor, administered in 3-week cycles (Schedule 2/1). Br J Cancer. 2011; 104:1862–8. [PubMed: 21610706]
13. Finn R, Crown J, Lang I, Boer K, Bondarenko I, Kulyk S. Results of a randomized phase 2 study of PD 0332991, a cyclin-dependent kinase (CDK) 4/6 inhibitor, in combination with letrozole vs letrozole alone for first-line treatment of ER+/HER2– advanced breast cancer (BC). Cancer Res. 2012; 72(3)
14. Dick FA, Sailhamer E, Nicholas J. Mutagenesis of the pRB Pocket Reveals that Cell Cycle Arrest Functions Are Separable from Binding to Viral Oncoproteins. Mol Cell Biol. 2000; 20:3715–27. [PubMed: 10779361]
15. Huillard E, Hashizume R, Phillips JJ, Griveau A, Ihrie RA. Cooperative interactions of BRAF V600E kinase and CDKN2A locus deficiency in pediatric malignant astrocytoma as a basis for rational therapy. Proc Natl Acad Sci U S A. 2012; 109:8710–5. [PubMed: 22586120]
16. Kwong LN, Costello JC, Liu H, Jiang S, Helms TL, Langsdorf AE, et al. Oncogenic NRAS signaling differentially regulates survival and proliferation in melanoma. Nat Med. 2012; 18:1503–10. [PubMed: 22983396]
17. Hezel AF, Kimmelman AC, Stanger BZ, Bardeesy N, Depinho Ra. Genetics and biology of pancreatic ductal adenocarcinoma. Genes Dev. 2006; 20:1218–49. [PubMed: 16702400]
18. Jones S, Zhang X, Parsons DW, Lin JCH, Leary RJ, Angenendt P, et al. Core signaling pathways in human pancreatic cancers revealed by global genomic analyses. Science. 2008; 321:1801–6. [PubMed: 18772397]

19. Aguirre AJ, Bardeesy N, Sinha M, Lopez L, Tuveson Da, Horner J, et al. Activated Kras and Ink4a/Arf deficiency cooperate to produce metastatic pancreatic ductal adenocarcinoma. Genes Dev. 2003; 17:3112–26. [PubMed: 14681207]
20. Bardeesy N, Aguirre AJ, Chu GC, Cheng KH, Lopez LV, Hezel AF, et al. Both p16(Ink4a) and the p19(Arf)-p53 pathway constrain progression of pancreatic adenocarcinoma in the mouse. Proc Natl Acad Sci U S A. 2006; 103:5947–52. [PubMed: 16585505]
21. Schutte M, Hruban RH, Geradts J, Maynard R, Hilgers W, Rabindran SK, et al. Abrogation of the Rb / p16 Tumor-suppressive Pathway in Virtually All Pancreatic Carcinomas. Cancer Res. 1997:3126–30. [PubMed: 9242437]
22. Garnett MJ, Edelman EJ, Heidorn SJ, Greenman CD, Dastur A, Lau KW, et al. Systematic identification of genomic markers of drug sensitivity in cancer cells. Nature. 2012; 483:570–5. [PubMed: 22460902]
23. Boik JC, Narasimhan B. An R Package for Assessing Drug Synergism/Antagonism. J Stat Softw. 2010; 34
24. Carboni JM, Wittman M, Yang Z, Lee F, Greer A, Hurlburt W, et al. BMS-754807, a small molecule inhibitor of insulin-like growth factor-1R/IR. Mol Cancer Ther. 2009; 8:3341–9. [PubMed: 19996272]
25. Pollak M. The insulin and insulin-like growth factor receptor family in neoplasia: an update. Nat Rev Cancer. 2012; 12:159–69. [PubMed: 22337149]
26. Eser S, Reiff N, Messer M, Seidler B, Gottschalk K, Dobler M, et al. Selective Requirement of PI3K/PDK1 Signaling for Kras Oncogene-Driven Pancreatic Cell Plasticity and Cancer. Cancer Cell. 2013:406–20. [PubMed: 23453624]
27. Dimri GP, Lee X, Basile G, Acosta M, Scott G, Roskelley C, et al. A biomarker that identifies senescent human cells in culture and in aging skin in vivo. Proc Natl Acad Sci U S A. 1995; 92:9363–7. [PubMed: 7568133]
28. Comstock CES, Augello Ma, Goodwin JF, de Leeuw R, Schiewer MJ, Ostrander WF, et al. Targeting cell cycle and hormone receptor pathways in cancer. Oncogene. 2013:1–11.
29. Collado M, Serrano M. Senescence in tumours: evidence from mice and humans. Nat Rev Cancer. 2010; 10:51–7. [PubMed: 20029423]
30. Kennedy AL, Morton JP, Manoharan I, Nelson DM, Jamieson NB, Pawlikowski JS, et al. Activation of the PIK3CA/AKT pathway suppresses senescence induced by an activated RAS oncogene to promote tumorigenesis. Mol Cell. 2011; 42:36–49. [PubMed: 21474066]
31. Carrière C, Gore aJ, Norris AM, Gunn JR, Young AL, Longnecker DS, et al. Deletion of Rb accelerates pancreatic carcinogenesis by oncogenic Kras and impairs senescence in premalignant lesions. Gastroenterology. 2011; 141:1091–101. [PubMed: 21699781]
32. Guha M. Anticancer IGF1R classes take more knocks. Nat Rev drug Discov. 2013; 12:754807.
33. Elkabets M, Vora S, Juric D, Morse N, Mino-Kenudson M, Muranen T, et al. mTORC1 Inhibition Is Required for Sensitivity to PI3K p110α Inhibitors in PIK3CA-Mutant Breast Cancer. Sci Transl Med. 2013; 5:196ra99.
34. Corcoran RB, Rothenberg SM, Hata AN, Faber AC, Piris A, Nazarian RM, et al. TORC1 Suppression Predicts Responsiveness to RAF and MEK Inhibition in BRAF-Mutant Melanoma. Sci Transl Med. 2013; 5:196ra98.
35. Zacharek SJ, Xiong Y, Shumway SD. Negative regulation of TSC1-TSC2 by mammalian D-type cyclins. Cancer Res. 2005; 65:11354–60. [PubMed: 16357142]
36. Miller ML, Molinelli EJ, Nair JS, Sheikh T, Samy R, Jing X, et al. Drug Synergy Screen and Network Modeling in Dedifferentiated Liposarcoma Identifies CDK4 and IGF1R as Synergistic Drug Targets. Sci Signal. 2013; 6:ra85. [PubMed: 24065146]
37. Ciriello G, Miller ML, Aksoy BA, Senbabaoglu Y, Schultz N, Sander C. Emerging landscape of oncogenic signatures across human cancers. Nat Genet. 2013; 45:1127–33. [PubMed: 24071851]

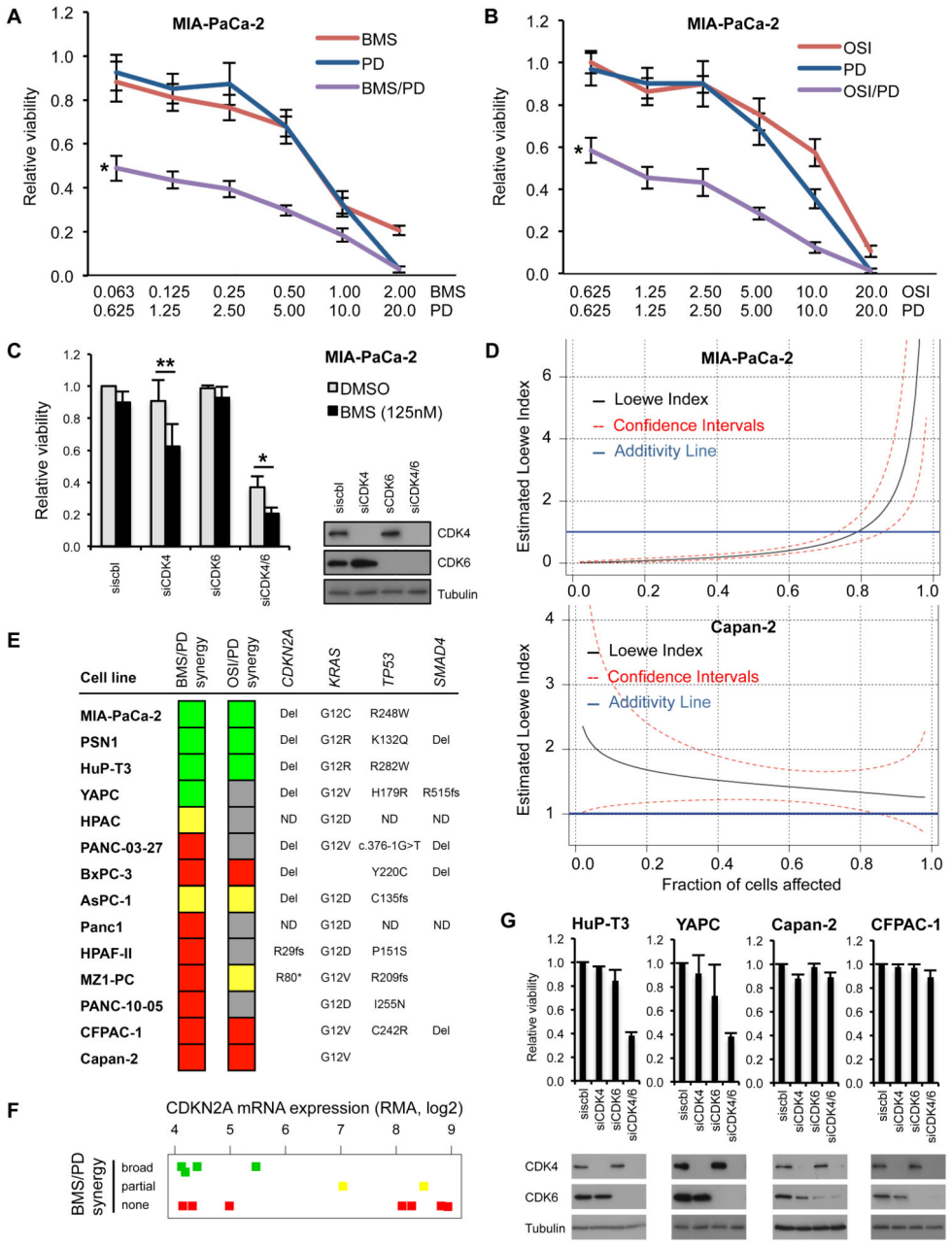

Figure 1. CDK4/6 and IGF1R/IR inhibitors synergize to reduce viability of PDAC cells with *CDKN2A* deletion

(A) MIA-PaCa-2 cells were treated with BMS-754807 (BMS), PD-0332991 (PD) or their fixed-ratio (1:10) combination (BMS/PD) over a concentration range (μM) for 72 h and cell viability was measured relative to DMSO treated controls.

(B) Relative viability of MIA-PaCa-2 cells treated with OSI-906 (OSI), PD-0332991 or their fixed-ratio (1:1) combination (OSI/PD).

(C) Relative viability of MIA-PaCa-2 cells treated with 125 nM BMS-754807 or DMSO after knockdown of CDK4 and/or CDK6 (siscbl, control siRNA). Data are means from at

least two independent replicates and error bars indicate s.e.m. for (A) through (C) (** $p<0.01$ and * $p<0.05$, one-tailed t test).

(D) Synergy plots for MIA-PaCa-2 or Capan-2 cells treated with BMS-754807, PD-0332991 or their fixed-ratio combination show Loewe indices per fraction of cells affected by the combination treatment: <1 indicates synergism, =1 indicates additivity (blue line) and >1 indicates antagonism with 95% confidence (red dashed lines) (N=2).

(E) Synergy analysis summary for the indicated PDAC cell lines treated with the BMS-754807/PD-0332991 or OSI-906/PD-0332991 combination. Green squares represent significant synergy over a broad effect range, yellow squares indicate significant synergy over less than 50% of the effect range and red squares show lack of significant synergy. Mutational status of cancer genes mutated in at least three of the tested cell lines are reported (Sanger COSMIC Cell Lines Project v65; ND not determined).

(F) *CDKN2A* mRNA expression (Broad-Novartis Cancer Cell Line Enzyclopedia database) in PDAC cell lines with broad (green), partial (yellow) or no (red) synergy of BMS-754807 and PD-0332991.

(G) Viability (mean +/- s.d., relative to siscbl control) of HuP-T3, YAPC, Capan-2, and CFPAC-1 cells 6 days after transfection with CDK4 and/or CDK6 siRNA.

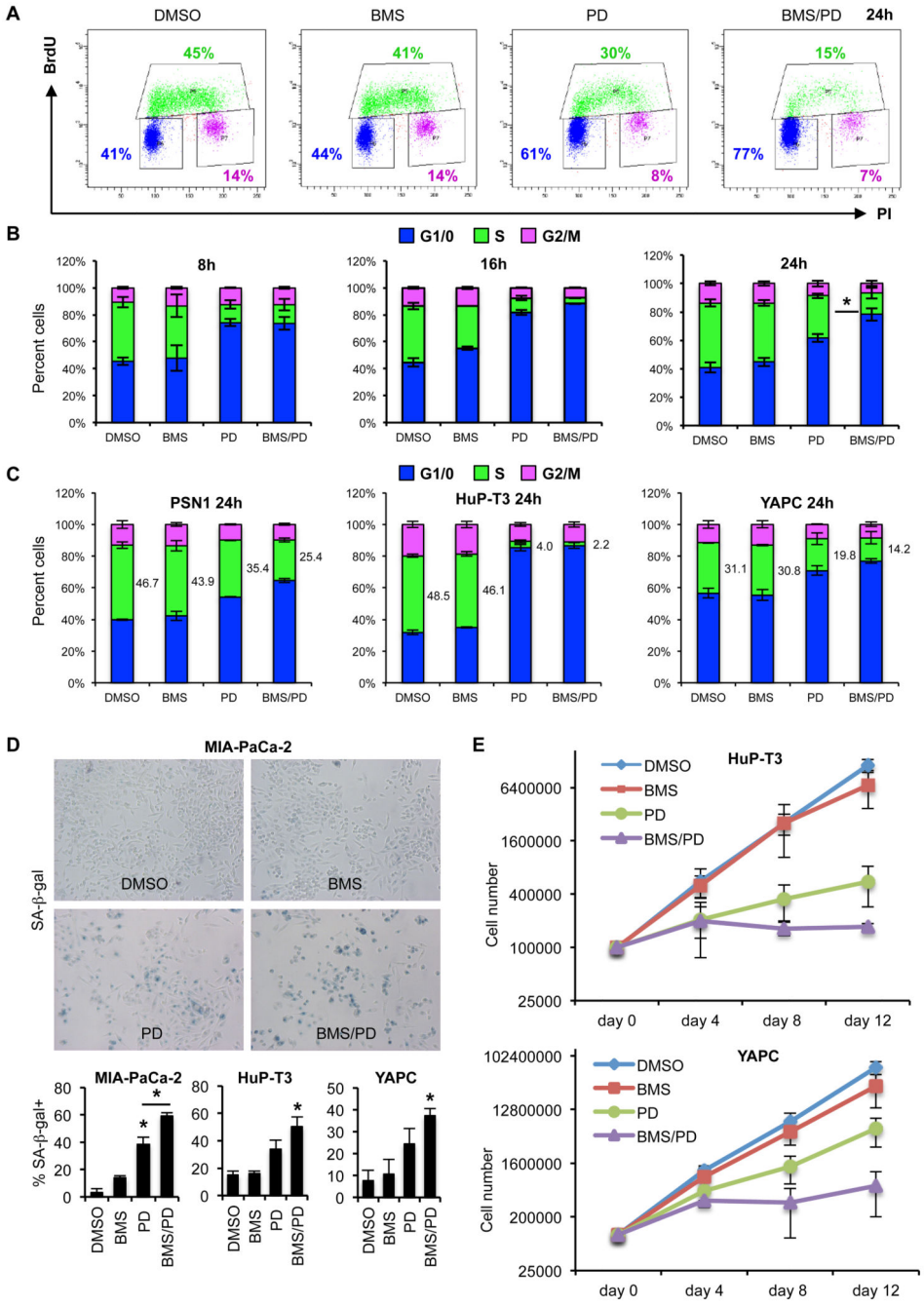

Figure 2. The combination of PD-0332991 and BMS-754807 enhances G1 arrest and senescence

(A) Bivariate flow cytometry analyses of MIA-PaCa-2 cells treated 24 h with 50 nM BMS-754807 (BMS), 500 nM PD-0332991 (PD), their combination (BMS/PD, 50 nM/500 nM) or DMSO. The x-axis denotes DNA content as detected with PI, the y-axis shows cells undergoing active S-phase as indicated by BrdU labeling. Inset values show percent cells in G1/0, S, and G2/M phase.

(B) MIA-PaCa-2 cells were treated for 8 h, 16 h, and 24 h as described in (A). Bar graphs show percent cells in G1/0, S, and G2/M phase as determined by BrdU/PI staining (N=2, * $p<0.05$, two-tailed t test).
(C) PSN1, HuP-T3, and YAPC cells were treated for 24 h and analyzed as in (A) and (B).
(D) Senescence-associated β-galactosidase (SA-β-gal) staining of MIA-PaCa-2, HuP-T3, and YAPC cells treated for 72 h as described in (A). Images are representative of the MIA-PaCa-2 staining. Bar graphs show mean percentage of SA-β-gal positive cells (* $p<0.05$, two-tailed t test).
(E) Population doubling of HuP-T3 and YAPC cells that were continuously cultured for 12 days in BMS-754807, PD-0332991, their combination or DMSO and counted every four days. Data are from two independent replicate assays and error bars represent s.d. for all experiments.

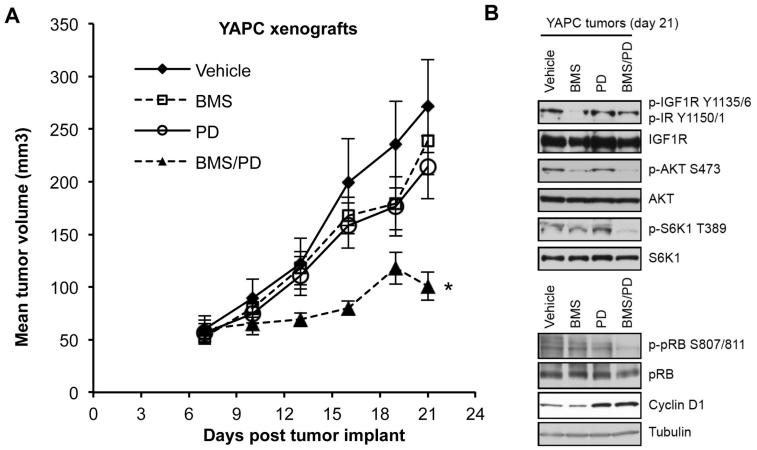

Figure 3. Concurrent treatment with PD-0332991 and BMS-754807 is synergistic *in vivo*

(A) YAPC xenografts were treated with 15 mg/kg BMS-754807 (BMS) (N=5), 75 mg/kg PD-0332991 (PD) (N=6), their combination (BMS/PD) (N=5) or vehicle (N=5) on days 8, 10, 12, 14, 17, 19, and 21 after subcutaneous tumor implant and tumor volumes (mean +/- s.e.m) were measured every three days from day 7. p values were calculated by two-tailed t test for BMS/PD versus the other groups (* $p<0.05$) and the single agent treatments versus the vehicle group (not significant).

(B) Tumors were lysed following completion of the treatment study and analyzed by Western blotting with the indicated antibodies; a representative of at least two independent experiments is shown.

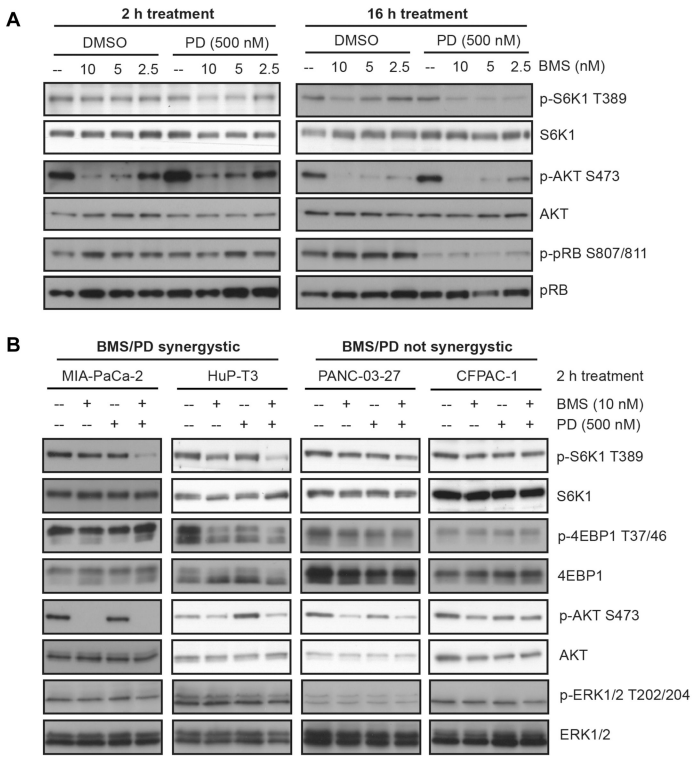

Figure 4. The drug combination inhibits S6K1 in the sensitive PDAC cell lines

(A) PSN1 cells were treated for 2 h and 16 h with BMS-754807 (BMS) doses ranging from 2.5 to 10 nM in the presence of 500 nM PD-0332991 (PD) or DMSO, and the cell lysates were analyzed by Western blotting.

(B) The sensitive PDAC cell lines MIA-PaCa-2 and HuP-T3 and the insensitive cell lines PANC-03-27 and CFPAC-1 were treated for 2 h with 10 nM BMS-754807, 500 nM PD-0332991, their combination or DMSO, and cell lysates were probed with the indicated antibodies.

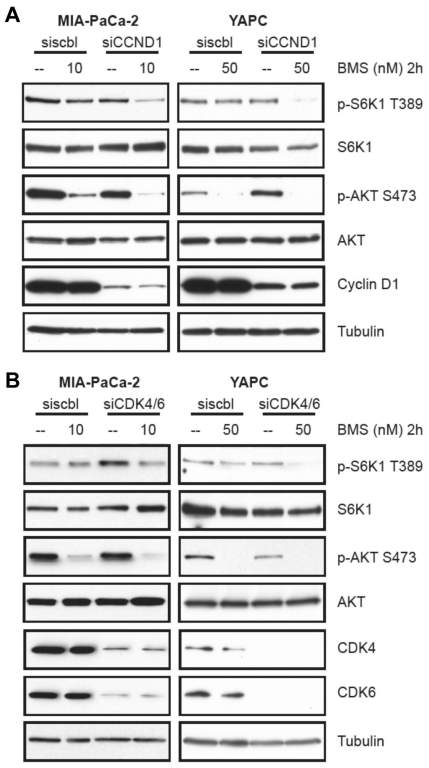

Figure 5. Knockdown of Cylin D1 or CDK4/6 sensitizes PDAC cells to S6K1 inhibition by BMS-754807

(A) MIA-PaCa-2 and YAPC cells were transfected with siRNA targeting Cyclin D1 (siCCND1), or control siRNA (siscbl). After 72 h, the cells were treated for 2 h with BMS-754807 (BMS) or DMSO control, and cell lysates were analyzed for the indicated proteins.

(B) CDK4/6 were depleted with siRNA (siCDK4/6) for 72 h, followed by 2 h treatment with BMS-754807 or DMSO and Western blotting.

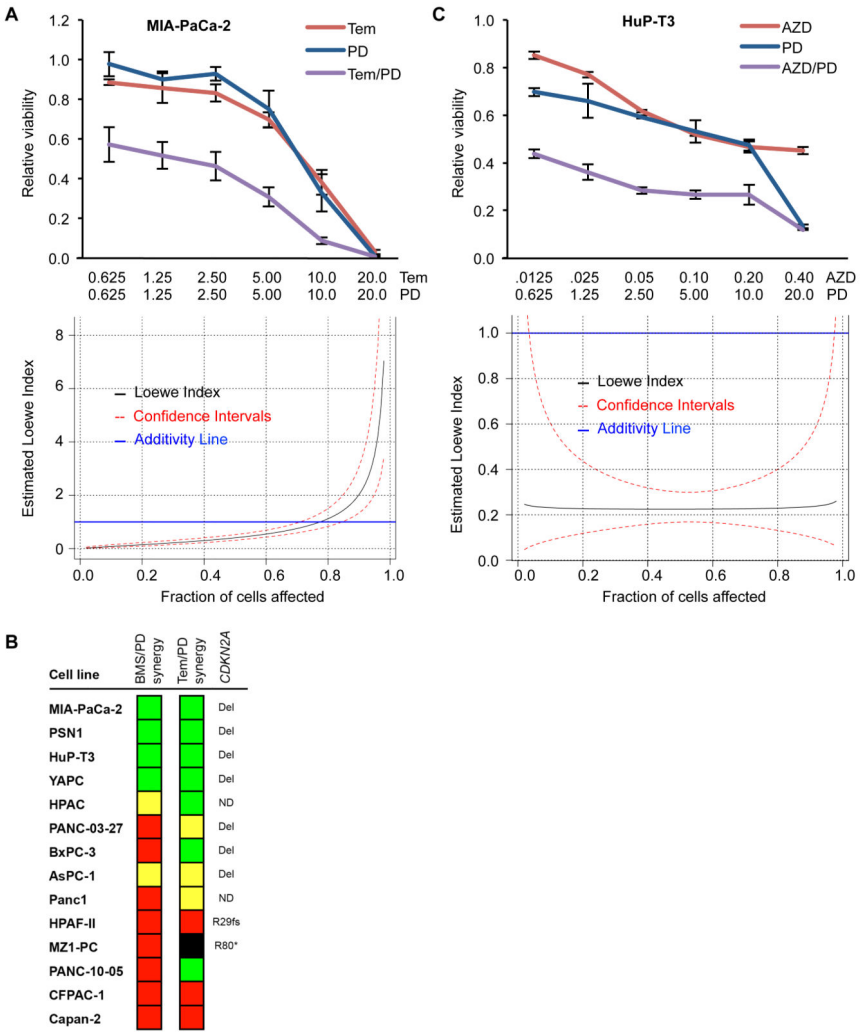

Figure 6. PD-0332991 synergizes with mTOR inhibitors to inhibit the growth of PDAC cell lines

(A) Relative viability (mean +/- s.e.m.) of MIA-PaCa-2 cells treated for 72 h with temsirolimus (Tem), PD-0332991 (PD) or their fixed-ratio (1:1) combination (Tem/PD) over a concentration range (μM). Synergy plot shows Loewe indices per fraction of cells affected by the combination treatment: <1 indicates synergism, =1 indicates additivity (blue line) and >1 indicates antagonism with 95% confidence (red dashed lines).

(B) Synergy analysis summary for the indicated PDAC cell lines and the temsirolimus/ PD-0332991 combination (N=2): Green squares represent significant Loewe synergy over a broad effect range, yellow squares indicate significant synergy over less than 50% of the effect range and red squares show lack of significant synergy. BMS-754807/PD-0332991 synergy analysis from Figure 1E was included for comparison.

(C) Relative viability (mean +/- s.e.m.) of HuP-T3 cells treated with AZD-8055 (AZD), PD-0332991 or their fixed-ratio (1:50) combination (AZD/PD). Synergy plot shows Loewe indices per fraction of cells affected by the combination treatment.

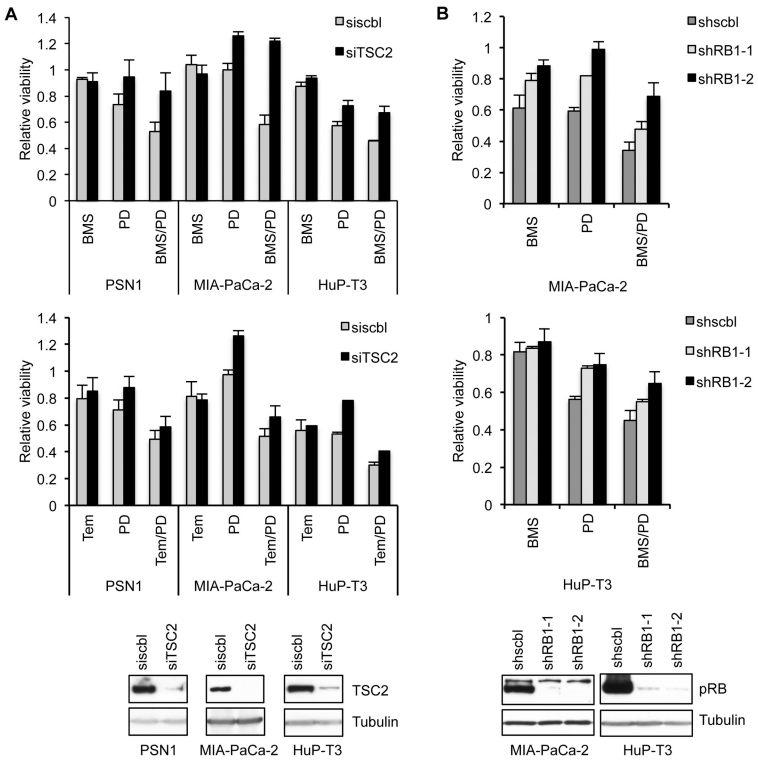

Figure 7. TSC2 or pRB depletion restores growth in the presence of CDK4/6 and IGF1R/IR inhibitors

(A) Relative viability of PSN1, MIA-PaCa-2, or HuP-T3 cells treated with 0.25 μM BMS-754807 (BMS), 2.5 μM temsirolimus (Tem), 2.5 μM PD-0332991 (PD), or their combinations (BMS/PD and Tem/PD) after knockdown of TSC2 (siscbl, control siRNA). (B) MIA-PaCa-2 and HuP-T3 cells were infected with two different short hairpin RNAs targeting RB1 (shRB1-1, shRB1-2) or control shRNA (shscbl). After puromycin selection, cells were treated for 72 h with 0.25 μM BMS-754807, 2.5 μM PD-0332991, or their combination. Error bars represent s.e.m. for all experiments.